Ecotoxicity Assessment of Photoinduced Imidacloprid Degradation Using HPLC-HRMS, QSAR and Ecotoxicity Equivalents

Melanie Voigt
Niederrhein University of Applied Sciences: Hochschule Niederrhein
Victoria Langerbein
Niederrhein University of Applied Sciences: Hochschule Niederrhein
Martin Jaeger (martin.jaeger@hs-niederrhein.de)
Niederrhein University of Applied Sciences https://orcid.org/0000-0002-7709-2869

Research Article

Keywords: Imidacloprid, HPLC-HRMS, ecotoxicity, QSAR, radical scavenger, AOPs

Posted Date: December 15th, 2021

DOI: https://doi.org/10.21203/rs.3.rs-1131873/v1

Abstract

Background

Imidacloprid is among the most widely used insecticides and today is found in surface and ground water worldwide. Together with four other neonicotinoids, it has been registered in the EU watchlist for monitoring. To prevent imidacloprid from entering water bodies, Advanced Oxidation Processes have been intensely researched. Photoirradiation proved one of the most efficient methods to degrade and eliminate anthropogenic micropollutants from waters. Their ecotoxicity assessment of photoinduced degradation and transformation products especially in the absence of reference standards is still heavily explored.

Results

In this study, UVA and UVC irradiation in combination with titanium dioxide P25 as photocatalyst were investigated for their degrading and eliminating effects and effectiveness on imidacloprid. Humic acid was used as natural organic matter additive. High-performance liquid chromatography coupled with high-resolution and higher order mass spectrometry allowed to identify and monitor imidacloprid and its degradation intermediates yielding seven new structures and concentration-time (*c-t*) profiles. The correlation of structures and the application of radical scavengers and photocatalyst helped distinguish between direct photoinduced and indirect hydroxyl-radical induced degradation mechanisms. Only imidacloprid-urea and desnitro-imidacloprid resulted from direct degradation, all other products from the indirect mechanism. The ecotoxicity of all identified compounds was assessed by quantitative structure activity relationship (QSAR) analysis. Ecotoxicity equivalents (ETEs) were introduced allowing a classified ranking of the products and an assessment of the overall hazardous potential of the irradiated solution at a given moment. Generally, the number of hydroxyl substituents was inversely correlated to ecotoxicity due to a single product. From the *c-t* curves, time-dependent ETE profiles were established.

Conclusions

Structure elucidation and *c-t* profiles from liquid chromatography-high resolution mass spectrometry allowed to distinguish between direct and indirect degradation mechanisms. Structure specific ecotoxicity assessment could be achieved through QSAR analysis. Ecotoxicity hazard was ranked based on ETEs. The time-dependent ETE profile proved suitable to reflect the effect of irradiation duration and allow to estimate the irradiation time required to eliminate ecotoxicity, which may be relevant for potential applications in wastewater treatment plants.

Background

Regular monitoring and random sampling have revealed today's ubiquitousness of anthropogenic micropollutants, such as pharmaceuticals or pesticides, in lakes and river waters [1–3]. This situation urged the European commission to introduce a watchlist of particularly hazardous chemical substances

[4, 5]. Still, too little information has been available about the distribution of these substances. Each country of the European Union has hence been obliged to collect monitoring data for these substances and map their distribution and concentrations in water bodies. The current second EU watchlist comprises five neonicotinoids, among them imidacloprid [5]. Neonicotinoids act as neurotoxins and possess high ecotoxicity against arthropods and aquatic organisms [6]. They are also highly persistent and cannot be removed from soils and water. [7] Imidacloprid occurs in European surface waters of France, Germany and Spain, but also of Australia, Brazil, Burkina Faso, China, Kenya and the USA with concentrations from ng L^{-1} to 3 µg L^{-1} [8]. As main entry routes into open waters, agriculture and sewage systems have been recognized [6]. Sewage treatment plants are no longer capable of complete elimination [3, 9–11].

To effectively remove micropollutants, advanced purification processes have been researched for years including Advanced Oxidation Processes (AOPs), whose common feature is the occurrence of hydroxyl radicals [12–14]. Among others, hydroxyl radicals can be generated from water through UVC irradiation [15]. Yet, UV radiation may excite compounds followed by chemical reactions. Both pathways leading to transformation and degradation have referred to as the direct degradation mechanism and - in case of hydroxyl radical induction - the indirect one [8, 16]. The direct mechanism is governed by the absorption spectrum of the compound and the emission spectrum of the lamp. For the generation of hydroxyl radicals UVC radiation or UVA light and a suitable photocatalyst such as titanium dioxide are required [17, 18]. Attempts were made to distinguish between both degradation mechanisms [8, 16, 19]. In this respect, radical scavengers such as tert-butanol and methanol suppress hydroxyl radical-induced oxidation.[20–22]. Occasionally, degradation products from AOPs were suspected to be more toxic than the original substances [23, 24]. During an AOP, the concentration-time (c-t) curves were often monitored and the structures of degradation or transformation products were often elucidated by high performance-liquid chromatography (HPLC) coupled to high-resolution mass spectrometry (HRMS) and higher order mass spectrometry (MS^n)[25–28] As matrix, pure water or water containing natural organic matters such as humic acid and fulvic acid were used [29, 30].

Due to the lack of reference standards for photodegradation products, experimental determination of ecotoxicological parameters from assays with *Daphnia magna* or *Vibrio fisherii* have been rare or impossible. Quantitative Structure-Activity Relationship (QSAR) analysis is a fast and computer-based alternative for ecotoxicology assessment [31, 32]. Within QSAR, profiling is carried out first to assign the analyzed structures to a specific class, based on similarity according to the Simplified Molecular Input Line Entry Specification (SMILES) code [33]. Database comparison at this point may already yield ecotoxicological data if present. If not, two different models, that were derived from available *in vitro* and/or *in vivo* experimental data, can be employed: ECOSAR and the one introduced by Veith et al. and Pavan et al [34, 35]. Starting from these models, chemometric methods, such as linear or non-linear regressions, are eventually used to predict the ecotoxic values for the structures under consideration.

In this study, the photoinduced degradation of imidacloprid was investigated using HPLC-HRMS and MS^n. The influence of irradiation with UVA and UVC light, the presence of titanium dioxide, tert-butanol

and humic acid on the degradation and transformation were studied with respect to chemical kinetics and structures of the resulting products. From the combined analysis of the c-t curves and chemical structures, mechanistic distinction between direct absorption-induced degradation and indirect hydroxyl radical-induced transformation was aimed at. To assess ecotoxicity, the identified intermediates and products were submitted to QSAR analysis. Transformation of obtained ecotoxicity values to ecotoxicity equivalents (ETEs) for all products led to a ranking with respect to the hazardous potential. The ETEs were also correlated with the *c-t* curves to yield time-dependent ETEs.

Methods

Chemicals and reagents

For all photoinduced degradation experiments imidacloprid (≥98.0%, Sigma-Aldrich, Steinheim, Germany) was used. Imidacloprid was dissolved in ultrapure water (Berrytec, Grünwald, Germany) with a final concentration of 20 mgL^{-1}. For radical scavenging experiments, *tert*-butanol (99.5%, Acros Organics, Geel, Belgium) was added to the solution to yield final concentrations of 5% and 20%. As photocatalyst, 100 mg of TiO_2 P25 (Acros Organics, Geel, Belgium) were suspended. Other solutions were prepared by adding 5 mg of humic acid (Alfa Aesar, Haverhill, Massachusetts, USA).

Absorption spectra

Absorption spectra were recorded from 200 to 1100 nm using a UV5Nano spectrometer (Mettler Toledo, Columbus, USA). Emission spectra of the UV lamps were recorded using a HR4000 spectrometer (Ocean Optics, Duiven, The Netherlands).

Photoinduced degradation experiments

All photoinduced degradation experiment were performed in a 1 L batchreactor (Peschl Ultraviolett, Mainz, Germany), covered with aluminum foil. Two different light sources were used: a medium-pressure mercury lamp (Heraeus, TQ 150, 150 W) for UVA radiation, that was operated with a water cooling system, and an low-pressure mercury lamp (Heraeus TNN 15/32, 15 W) emitting UVC radiation, that was operated without cooling. Both lamps emitted polychromatic light. The maximum intensities were at 313, 365, 405, 437, 547, 578 and 580 nm. The UVC lamp emitted additionally at 185 nm and 254 nm. The total flux of photons in the wavelength range between 200 and 500 nm was determined using ferrioxalate actinometry according to IUPAC [36, 37]. The flux amounted to 3.50 mmol min^{-1} L^{-1} for the UVA lamp and to 2.03 mmol min^{-1} L^{-1} for the UVC lamp. The UVA lamp was allowed to reach working temperature over 2 min, while the UVC lamp did not require pre-heating. The UV lamps were inserted into the center of the reactor. A magnetic stirrer 500 rpm was used to ensure thorough mixing in the reactor. The reaction temperature in the entire reactor amounted to 22 ± 2 ° C and was checked during the photoinduced degradation experiment using a thermometer. All solutions were irradiated for 10 minutes with UVA or UVC light. Samples of 2 mL were taken from the reactor at 30 s intervals during the first 5 min of

irradiation and at one minute intervals for the remaining 5 min. The samples were transferred to HPLC-HRMS analysis.

HPLC-HRMS analysis

Reversed-phase chromatographic analysis was performed using an Eclipse Plus C18 (ZORBAX, 3.5 µm, 2.1x150 mm, Agilent, Waldbronn, Germany). The chromatography was performed at a flow rate of 0.3 mL min^{-1} at a column temperature of 40°C. As eluents ultrapure water (A) and acetonitrile (B) (Carl Roth, Karlsruhe, Germany) were used, both acidified with 0.1% formic acid (Fluka-Honeywell; Seelze, Germany). Elution started with eluents A and B varying from 99:1 to 70:30 within 1 min, followed by isocratic conditions A:B 25:75 during the next 10 min. At 11.1 min the solvent composition was set to 1:99 and held for 0.1 min. At minute 15 the gradient was reset to starting conditions continuing for further 15 minutes. The overall chromatographic run-time amounted to 20 min. The injection volume was 5 µL.

For accurate mass determination, recording of concentration-time (*c-t*) curves, and MS^n experiments, an electron spray ionization quadrupole ion trap orbitrap (ESI-Q-IT-OT) (Orbitrap IDX, ThermoFisher Scientific, Waltham, USA) coupled to an ultra-high performance liquid chromatography (UHPLC) system (Vanquish, ThermoFisher Scientific, Waltham, USA) was used. The mass range was set from 100 to 2000 m/z for all experiments. Fragmentation was performed in the higher-energy collision-induced dissociation (HCD) cell using collision energies of 30% for MS^2 and 45% for MS^3. The spray voltage was set to 3500 V. The vaporizer and ion transfer tube temperature was 300°C. Instruments were controlled with Thermo Scientific Xcalibur Version 4.3.73.11.

Kinetics of photodegradation

Concentration-time curves and kinetic profiles of the photoinduced degradation of imidacloprid and its transformation and degradation products were computed using the curve fitting toolbox within the software MatLab R2018a (MathWorks, Natick, MA, USA). Mathematical treatment followed chemical kinetics as described in detail in previous studies. [26, 27, 38–40]

QSAR

The QSAR analysis was carried out using the OECD QSAR toolbox Version 4.3.1 (OECD, Paris, France). First, the chemical structure formulae of imidacloprid and its transformation and degradation products were sketched using ACD/ChemSketch 2016.1.1 (ACDLabs, Toronto, ON, Canada) software and imported into the QSAR toolbox. Two models were used: Firstly, Ecological Structure Activity Relationship (ECOSAR), secondly the model according to Veith et al. in its revised form by Pavan et al. [34, 35]. As relevant value, the acute toxicity (LC_{50}) of *Pimephales promelas* (fathead minnow) was chosen. From the four calculation models for *P. promelas* in the QSAR toolbox the following descriptors were used. The log k_{ow} value and the LUMO energy were applied for the first model (M1). For models 2 to 4 (M2 to M4), only the log k_{ow} value was relevant as descriptor.

Within ECOSAR, the chemical structures were employed in the SMILES representation. Depending on the SMILES combination, the chemical substances were assigned to different classes. To this purpose, a profiling was carried out to evaluate the relevant ECOSAR classes for imidacloprid and its degradation products. Suitable classes were selected for further analysis. Chronic toxicity as chronic value (ChV) and acute toxicity as lethal concentration, 50% (LC_{50}) and half maximal effective concentration (EC_{50}) were predicted. As organisms, *Daphnia* (Branchiopoda), fish (Actinopterygii) and green algae were chosen.

Time-dependent ecotoxicity equivalents

Toxicity ranking for the initial compound and the transformation products was created according to the ecotoxicty values obtained from QSAR analysis. Following the ranking order, values 1 to 14 from least to most toxic were assigned to the structures. These assigned values were multiplied by the MS peak area. The resulting values were added for all products found in the sample at a given time. Values were normalized to the initial ecotoxicity, referred to as ecotoxicity equivalents, cf. equation (1). Time-dependent ecotoxicity representations were obtained as the time course of the normalized values for a given sample.

Results And Discussion

It is important to prevent imidacloprid from entering surface waters to minimize its ecotoxicological hazard. With respect to researched fourth purification stages and their efficiency, the photoinduced degradation of imidacloprid was investigated and related to ecotoxicological potential. Firstly, different conditions were probed to yield a cross section of effects on photoinduced degradation. The corresponding concentration-time curves from normalized mass-area are shown in Figure 1. For mechanistic interpretations, the UVA and UVC lamps emission spectra and the absorption spectrum of imidacloprid are given in Figure 1 as well.

From the concentration-time profiles, it can be recognized that in general UVC radiation caused a faster and more complete degradation of imidacloprid. The additives humic acid, *tert*-butanol did not exercise large velocity influences on the degradation. In most cases, imidacloprid was degraded within 10 minutes under UVC irradiation. Under UVA irradiation, only a very weak degradation was observed. Only the addition of the photocatalyst TiO_2 achieved acceleration, while tert-butanol led to deceleration. Incomplete degradation was observed under all conditions of UVA irradiation during 10 min in contrast to UVC irradiation. Kinetic rate constants k and half-lives $t_{1/2}$ determined from the degradation curves are collected in Table 1.

Table 1
Photoinduced degradation rate-constants and half-lives of imidacloprid.

Irradiation source	Additives	k/min^{-1}	$t_{1/2}$/min
UVA	-	6.1E-02	1.1E+01
	5% tert-butanol	5.1E-03	1.4E+02
	100 mg TiO_2 P25	1.8E-01	3.9E+00
UVC	-	6.6E-01	1.1E+00
	5% tert-butanol	5.8E-01	1.2E+00
	20% tert-butanol	5.6E-01	1.2E+00
	5 mg humic acid	4.6E-01	1.5E+00

The fastest degradation was observed under VUV/UVC irradiation in pure water. The degradation rate constant was determined as 6.6E-01 min^{-1}, which was found in a good agreement with a previous study reporting 6.7E-01 min^{-1} [6]. The addition of *tert*-butanol and humic acid decelerated the degradation of imidacloprid only slightly. Tert-butanol is a known radical scavenger and as such able to intercept the hydroxyl radicals that are formed through VUV/UVC radiation. Since UVA radiation did not lead to degradation or transformation, it can be concluded that the wavelength 254 and 185 nm were essential for imidacloprid elimination [8]. As the TiO_2 catalyzes the formation of hydroxyl radicals under UVA irradiation, imidacloprid was found to vanish under these conditions. The contribution of hydroxyl radicals was diminished by the presence of tert-butanol. Yet, even 20% of tert-butanol was not sufficient to completely suppress imidacloprid elimination. It could hence be assumed that photochemistry occurred, directly induced by the absorption of radiation at 254 nm. Humic acid, which was used to simulate natural organic matter in surface water, also absorbed and thus reduced the amount of light to induce imidacloprid reactions. As a consequence, elimination by UV irradiation under non-laboratory conditions will take longer than under model conditions.

It might be concluded that degradation through hydroxyl radical formation leads to faster transformation or degradation of imidacloprid than photochemistry by direct absorption. This finding was supported, since the addition of TiO_2 during UVA irradiation led to an elimination reaction constant in the same order of magnitude as during UVC irradiation, cf. Table 1.

The subsequent step was now to investigate whether a correlation of different conditions and hence different mechanisms with chemical structures could be observed. And whether the chemical structures might be found harmful to the aquatic environment.

Identified photoinduced degradation products

Among the photoinduced degradation and transformation products, the well-known imidacloprid derivatives 5OH-imidacloprid, desnitro-imidacloprid, desnitro-olefin-imidacloprid, urea-imidacloprid and olefin-imidacloprid were observed [41, 42]. Yet, many products were detected below an occurrence of 1% of the original substance. These products were hence excluded from further consideration. An overview of the most abundant products is shown in Table 2. The proposed structures all show the hydroxyl group at position 2 of the 6-membered ring. Using MS/MS and MS^n, the exact position of the hydroxyl group could not be determined from the fragmentation pattern. More detailed information on MS/MS and MS^n are given in the supplemental information table S1.

Table 2 Identified photoinduced degradation and transformation products of imidacloprid

Substance	RT /min	$[M+H]^+_{exact}$	$[M+H]^+_{accurate}$	Δ ppm	Proposedstructure	Reference
Imidacloprid	5.82	256.0596	256.0594	0.78	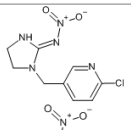	
Imi288	5.34	288.0494	288.0500	2.08	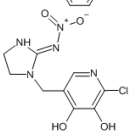	[41, 43–46]
Imi281	4.75		281.1166			This study
Imi272	5.00	272.0545	272.0546	0.37	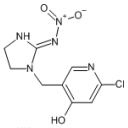	[41, 45–51]
Imi243a	3.79	243.0643	243.0643	0	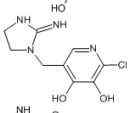	This study
Imi243b	3.95					
Imi228	4.79	228.0534	228.0531	1.32	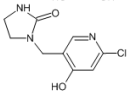	[50, 52]
Imi227	4.14	227.0694	227.0695	0.44	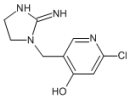	[42]
Imi226a	4.88	226.0378	226.0374	1.77	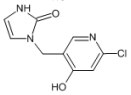	This study
Imi226b	4.80					
Imi225	4.29	225.0538	225.0539	0.44	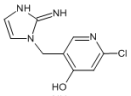	This study
Imi224	3.82	224.0697	224.0701	1.79	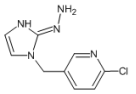	[43]
Imidacloprid-urea	4.22	212.0585	212.0586	0.47	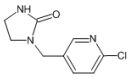	[41–43, 45–48, 50, 53–63]
Desnitro-imidacloprid	4.79	211.0745	211.0743	0.95	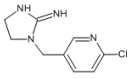	[41–43, 46, 53, 57, 59, 61, 63]
Desnitro-olefin-imidacloprid	4.01	209.0589	209.0593	0.48	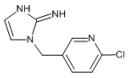	[41, 42, 48, 51]
Imi197	1.30		197.1034			This study
Imi194	3.98	194.0924	194.0923	0.52	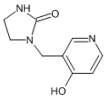	[42]
Imi193	2.00	193.1084	193.1082	1.04	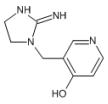	[42]

A total of 17 transformation or degradation products were identified. Five of them have not been reported before. Previous studies reported on the substance with m /z = 226 but described MS^n fragments different from those of this study, it can be assumed that these products were not identical [51]. Most of the identified products lacked the nitro group, except Imi272 and Imi288. When equal m/z values were observed at unequal retention times, e.g. Imi243a, b and Imi226a, b, the corresponding compounds were interpreted as regio-isomers with the hydroxyl group at different positions. Only, two substances, Imi243 and Imi281, could not be elucidated structurally. These were excluded from assessment of ecotoxicity.

In order to relate products to either the hydroxyl mechanism or the direct absorption mechanism, it is also interesting to classify the products to the conditions of the experiment. The classification and values referring to the percentage of the maximum of the c-t curve relative to the initial imidacloprid concentration are collected in Table 3. Concentration-time curves were recorded for all products. They are exemplarily shown for desnitro-imidacloprid and Imi194 in figure 2.

Table 3
Photo-induced degradation and transformation products of imidacloprid under different conditions; values refer to the percentage of the maximum of the *c-t* curve relative to initial imidacloprid concentration.

Substance	UVA /%	UVA+ 5% tert-butanol/%	UVA+ TiO_2 P25 /%	UVC /%	UVC + 5 mg humic acid /%	UVC + 5% tert-butanol /%	UVC + 20% tert- butanol /%
Imidacloprid	X	X	X	X	X	X	X
Imi288			1.8				
Imi281						6.3	9.3
Imi272			7.6				
Imi243a			1.4	1.4	1.5		
Imi243b			2.5				
Imi228				4.2	5.5		
Imi227				26.1	20.8	22.8	8.16
Imi226a				2.3	5.0		
Imi226b				1.0	1.7		
Imi225				2.3	2.3	8.9	
Imi224				2.1	6.7	8.4	2.3
Imidacloprid-urea				48.8	67.8	90.8	40.4
Desnitro-imidacloprid	6.1	7.0		21.4	39.6	64.6	
Desnitro-olefin-imidacloprid	7.0	6.7		4.2	4.7		
Imi197				1.2	1.8	2.1	
Imi194				3.1	3.0	7.5	1.5
Imi193				2.8	2.4	6.6	1.4

In case of UVA irradiation in the absence of TiO_2, only two products were identified with a proportion of more than 1%: desnitro-imidacloprid and desnitro-olefin-imidacloprid. Hence, these products should originate from direct absorption of UVA radiation and subsequent reactions. The lack of hydroxyl radical generating radiation led to the absence of the indirectly formed products, such as Imi227. Since imidacloprid was degraded only very little, few products at small abundance were expected.

In the presence of TiO_2, 4 products could be identified: Imi288, Imi272, Imi243a and Imi243b. From their chemical structure, it can be deduced that these transformation products involved hydroxyl substitution favored through the presence of photocatalyst.

Further products originated from VUV/UVC irradiation. The products Imi193, Imi194, imidacloprid-urea, Imi224, and Imi227 could be observed under all VUV/UVC irradiation conditions. It is rather obvious that the formation of hydroxyl radicals caused hydroxyl substitution at the pyridine moiety. Interestingly, the formation of the urea derivative seemed a consequence of UVC irradiation, under both hydroxyl radical formation and suppression conditions. Since the urea derivative did not occur under UVA irradiation in the presence of photocatalyst, distinction between the two mechanisms was not possible. The loss of the nitro group was found for a variety of conditions. The proportion of Imi193, Imi194, imidacloprid-urea, Imi224 and Imi227 decreased upon addition of more *tert*-butanol due to its radical scavenging capability.

The products Imi243, Imi226a, Imi226b and desnitro-olefin-imidacloprid were only observed under conditions with no tert-butanol. These products also stemmed from hydroxyl radical reactions. Addition of radical scavenger suppressed their formation as well. Yet, desnitro-imidacloprid, Imi225 and Imi197 were still observed at 5% tert-butanol, but disappeared at 20% tert-butanol. Desnitro-imidacloprid was likely to be formed via the direct mechanism as well, while 5% tert-butanol was sufficient to hamper the formation of Imi225, which possess the hydroxylated pyridine moiety and was hence considered due to the indirect mechanism. The higher content of tert-butanol eventually suppressed its formation.

The product Imi281 with unknown structure was only formed in the presence of tert-butanol, its proportion increasing with increasing amount of *tert*-butanol. This might suggest that this product originates from a reaction with *tert*-butanol.

The concentration-time curves of Imi194 and desnitro-imidacloprid are presented in figure 2. The profiles illustrate the different formation kinetics of the secondary products. The course of desnitro-imidacloprid was followed during UVA irradiation in water with 5% *tert*-butanol, during UVC irradiation in water, in water with 5% and 20% *tert*-butanol and in the presence of humic acid.

Degradation or transformation products whose concentration-time curve still increased after 10 minutes of UV exposure, such as Imi193 and Imi194, were observed. Other transformation products that were degraded again, such as the products Imi225 and Imi227, were found as well. They could be described as follow-up and subsequent-follow-up products.

Assessment of Ecotoxicity

For hydroxyl groups, six potential positions exist. For QSAR analysis, three positions were exemplarily investigated, i.e. 1, 2, and 3 as shown in Figure 3 for imidacloprid.

For the QSAR analysis based on ECOSAR, profiling yielded the structural classification. Best results were suggested when using the classes aliphatic amines and halopyridines, see Tables S2, S3 and S4 with representations of all possible isomers with respect to the hydroxyl group. The QSAR analysis was performed and ecotoxicity predicted. The resulting values are collected in Tables S5, S6 and S7.

QSAR results showed that ecotoxicity could be attributed to the positions within the molecule. A hydroxyl group at the pyridine ring, i.e. positions 2 and 3, had minor influence on the predicted values, such that only the isomer with the hydroxyl group in position 2 was considered further. When the hydroxyl substituent was located at the 5-membered ring, i.e. position 1, a lower value for ecotoxicity was calculated. A ranking of the identified structures according to ecotoxicity depending on positions 1 and 2 is displayed in Figure 4.

Among the imidacloprid transformation and degradation products, imidacloprid-urea, desnitro-imidacloprid, desnitro-olefin and imidacloprid as initial compound were ranked as the most ecotoxic substances against organisms from the aquatic environment. These compounds were not hydroxylated, but were detected under hydroxyl radical generating conditions as well, cf. Table 3 and above. Imidacloprid-urea was formed only during UVC irradiation. Its degradation was hampered in the presence of radical scavengers. The observation suggests that degradation was favored by hydroxyl radicals. In combination with the QSAR results, it might be concluded that ecotoxic effects could be reduced through hydroxyl substituents and secondary product elimination by hydroxyl radicals. According to QSAR analysis, the position of the hydroxyl group did not have a predominant effect. The number of hydroxyl substituents in contrast exercised a positive effect: The more hydroxyl groups the less ecotoxic the transformation product was predicted. The loss of the chlorine substituent was associated with a decrease in ecotoxicity.

Up to this point, the ecotoxicity was computed for each compound separately. Yet, the ecotoxicity is a function of irradiation time when conditions are kept constant. Hence, the total ecotoxicity of the solution was considered and computed as ecotoxicity equivalents (*ETE*) that are a function of irradiation time, cf. Equation 1 and Figure 5.

$$ETE(t) = \left[\sum_{n=1}^{n} \left(EQ * \mathrm{MSPeakArea}_A\right)\right](t) \,/\, ETE(t=0) \quad \text{eq. (1)}$$

where *n* is the number of identified products including imidacloprid, *EQ* the ecotoxicity ranking value resulting from QSAR analysis and *t* the irradiation time. The value of *ETE*(*t*=0) equals the QSAR value of imidacloprid.

As can be seen from Figure 5, UVA irradiation induced a steady decrease of ecotoxicity. Since only few degradation and transformation products were formed during UVA irradiation and their MS peak area remained very small as compared to that of imidacloprid, the predicted ecotoxicity resulted predominantly from imidacloprid. The ETE time-dependence equaled the degradation profile of imidacloprid, cf. Figure 5a). Upon addition of TiO_2 ETEs decayed faster, as was observed for imidacloprid as well.

Under VUV/UVC irradiation, the ecotoxicity initially increased both for imidacloprid in pure water and in the presence of 5% tert-butanol. The most transformation and degradation products were observed under these conditions; the profile of the ecotoxicity-time curves reflected the profile of the total product formation. At first, the ecotoxicity increased slowly, as did the number of observed products. Then, it decreased in the same way the products were eliminated again due to continuing VUV/UVC radiation. When the tert-butanol concentration amounted to 20%, the overall ecotoxicity decreased with irradiation time, since significantly fewer products were formed. Hence, imidacloprid had the greatest impact on the ecotoxicity under these conditions. The lowest overall ecotoxicity expressed in ETEs was achieved using UVA irradiation in the presence of 100 mg TiO_2 or using VUV/UVC irradiation in the presence of 20% *tert*-butanol.

The findings emphasize the importance of monitoring secondary products during UV irradiation. Too short a treatment might yield a mixture of intermediate products that might prove more ecotoxic than the initial substance. Using HRMS as detector, structural information could be obtained and used further for ecotoxicity prediction by QSAR. Monitoring all compounds was easily achieved by HRMS as well. Introducing ecotoxicity equivalents, the ecotoxicity of the total solution exposed to irradiation under different conditions could be assessed. These time-dependent ETEs could help better estimate efficacy and treatment times for elimination of hazardous substances.

Conclusions

The elimination of imidacloprid from model waters was accomplished through irradiation with UVC radiation and UVA light in the presence of the photocatalyst TiO_2 P25. Using HPLC-HRMS and MS^3, the degradation was monitored as c-t curves and the degradation and transformation products structurally characterized leading to the discovery of seven new transformation products. Degradation was traced back to the direct photo-induced, e.g. desnitro-imidacloprid, and the indirect hydroxyl radical-induced mechanism, e.g. Imi227, as supported by the identified structures. The distinction was supported by the experimental conditions, in particular presence and absence of TiO_2 during UVA irradiation and the scavenging of hydroxyl radicals by tert-butanol. Ecotoxicity was assessed by means of QSAR analysis based on the elucidated secondary products. Increasing number of hydroxyl groups due to the indirect mechanism and cleavage of the chlorine substituent were found to decrease ecotoxicity. Ecotoxicity values from QSAR were transformed into ETEs and an ecotoxicity ranking was established. Since transformation and degradation products were exposed to radiation and thus continued to react, time

dependent ETEs were introduced to reflect the overall ecotoxicity of the solution at a given moment. The ETE-time curve suggested an initial increase of ecotoxicity of an imidacloprid solution upon UVC irradiation followed by a significant removal, while UVA exposure led to a steady decrease. Irradiation times necessary for elimination may be better estimated from time-dependent ETEs. The presence of humic acid as NOM showed that irradiation with and without photocatalyst under real conditions would require longer duration but would still lead to successful degradation.

Abbreviations

AOPs Advanced Oxidation Processes

ChV Chronic Value

ECOSAR Ecological Structure Activity Relationships

ESI-Q-IT-OT electron spray ionization quadrupole ion trap orbitrap

EU European Union

c-t concentration-time

EC_{50} Half maximal effective concentration

ETE ecotoxicity equivalents

HCD higher-energy collision-induced dissociation

HPLC-HRMS high performance liquid chromatography-high resolution mass spectrometry

LC50 lethal concentration

LUMO Lowest Unoccupied Molecular Orbital

OECD Organization for Economic Co-operation and Development

QSAR Quantitative Structure-Activity Relationship

SMILES Simplified Molecular Input Line Entry Specification

UHPLC ultra-high performance liquid chromatography

UV ultraviolet

VUV vacuum-UV

Declarations

Ethics approval and consent to participate

Not applicable.

Consent for publication

Not applicable.

Availability of data and material

Data can be obtained upon request from the corresponding author. They will be made available via a link to the cloud Sciebo.

Competing interests

The authors declare that they have no competing interests

Funding

Open access funding provided by Niederrhein University of Applied Sciences.

Authors' contributions

MV: conceptualization**,** validation**,** data curation, experiments**,** writing **-** original draft **VL:** data curation**,** preparation, experiments **MJ:** formal analysis**,** writing **-** review and editing, supervision

Acknowledgments

The authors are grateful to Joachim Horst for technical support.

References

1. Kümmerer K (2009) Antibiotics in the aquatic environment - a review - part I. Chemosphere 75:417–34. https://doi.org/10.1016/j.chemosphere.2008.11.086
2. Syafrudin M, Kristanti RA, Yuniarto A, et al (2021) Pesticides in Drinking Water — A Review
3. Pietrzak D, Kania J, Malina G, et al (2019) Pesticides from the EU First and Second Watch Lists in the Water Environment. Clean - Soil, Air, Water 47:. https://doi.org/10.1002/clen.201800376
4. European Commission (2015) Commission Implementing Decision (EU) 2015/495 of 20 March 2015 establishing a watch list of substances for Union-wide monitoring in the field of water policy pursuant to Directive 2008/105/EC of the European Parliament and of the Council (notified under
5. European Commission (2018) Commission Implementing Decision (EU) 2018/840 of 5 June 2018 establishing a watch list of substances for Union-wide monitoring in the field of water policy pursuant to Directive 2008/105/EC of the European Parliament and of the Council and repealing Comm

6. Goulson D (2013) An overview of the environmental risks posed by neonicotinoid insecticides. J Appl Ecol 50:977–987. https://doi.org/10.1111/1365-2664.12111
7. Anderson JC, Dubetz C, Palace VP (2015) Neonicotinoids in the Canadian aquatic environment: A literature review on current use products with a focus on fate, exposure, and biological effects. Sci Total Environ 505:409–422. https://doi.org/10.1016/j.scitotenv.2014.09.090
8. Voigt M, Jaeger M (2021) Structure and QSAR analysis of photoinduced transformation products of neonicotinoids from EU watchlist for ecotoxicological assessment. Sci Total Environ 751:141634. https://doi.org/10.1016/j.scitotenv.2020.141634
9. Yi X, Zhang C, Liu H, et al (2019) Occurrence and distribution of neonicotinoid insecticides in surface water and sediment of the Guangzhou section of the Pearl River, South China. Environ Pollut 251:892–900. https://doi.org/10.1016/j.envpol.2019.05.062
10. Barbosa MO, Moreira NFF, Ribeiro AR, et al (2016) Occurrence and removal of organic micropollutants: An overview of the watch list of EU Decision 2015/495. Water Res 94:257–279. https://doi.org/10.1016/j.watres.2016.02.047
11. Sousa JCG, Ribeiro AR, Barbosa MO, et al (2018) A review on environmental monitoring of water organic pollutants identified by EU guidelines. J Hazard Mater 344:146–162. https://doi.org/10.1016/j.jhazmat.2017.09.058
12. Coha M, Farinelli G, Tiraferri A, et al (2021) Advanced oxidation processes in the removal of organic substances from produced water: Potential, configurations, and research needs. Chem Eng J 414:128668. https://doi.org/10.1016/j.cej.2021.128668
13. Mazivila SJ, Ricardo IA, Leitão JMM, Esteves da Silva JCG (2019) A review on advanced oxidation processes: From classical to new perspectives coupled to two- and multi-way calibration strategies to monitor degradation of contaminants in environmental samples. Trends Environ Anal Chem 24:1–10. https://doi.org/10.1016/j.teac.2019.e00072
14. Deng Y, Zhao R (2015) Advanced Oxidation Processes (AOPs) in Wastewater Treatment. Curr Pollut Reports 1:167–176. https://doi.org/10.1007/s40726-015-0015-z
15. Zoschke K, Börnick H, Worch E (2014) Vacuum-UV radiation at 185 nm in water treatment-a review. Water Res 52:131–45. https://doi.org/10.1016/j.watres.2013.12.034
16. Zhang Y, Zhang J, Xiao Y, et al (2017) Direct and indirect photodegradation pathways of cytostatic drugs under UV germicidal irradiation: Process kinetics and influences of water matrix species and oxidant dosing. J Hazard Mater 324:481–488. https://doi.org/10.1016/j.jhazmat.2016.11.016
17. Chávez AM, Ribeiro AR, Moreira NFF, et al (2019) Removal of organic micropollutants from a municipal wastewater secondary effluent by UVA-LED photocatalytic ozonation. Catalysts 9:. https://doi.org/10.3390/catal9050472
18. Al-Mamun MR, Kader S, Islam MS, Khan MZH (2019) Photocatalytic activity improvement and application of UV-TiO2 photocatalysis in textile wastewater treatment: A review. J Environ Chem Eng 7:. https://doi.org/10.1016/j.jece.2019.103248

19. Hensen B, Olsson O, Kümmerer K (2019) The role of irradiation source setups and indirect phototransformation: Kinetic aspects and the formation of transformation products of weakly sunlight-absorbing pesticides. Sci Total Environ 695:133808. https://doi.org/10.1016/j.scitotenv.2019.133808
20. Kozmér Z, Takács E, Wojnárovits L, et al (2016) The influence of radical transfer and scavenger materials in various concentrations on the gamma radiolysis of phenol. Radiat Phys Chem 124:52–57. https://doi.org/10.1016/j.radphyschem.2015.12.011
21. Wirzberger V, Klein M, Woermann M, et al (2021) Matrix composition during ozonation of N-containing substances may influence the acute toxicity towards Daphnia magna. Sci Total Environ 765:142727. https://doi.org/10.1016/j.scitotenv.2020.142727
22. Piechowski M von, Thelen M-A, Hoigne J, Bühler RE (1992) tert-Butanol as an OH-Scavenger in the Pulse Radiolysis of Oxygenated Aqueous Systems. Ber Bunsenges Phys Chem 96:1448–1454
23. Fatta-Kassinos D, Vasquez MI, Kümmerer K (2011) Transformation products of pharmaceuticals in surface waters and wastewater formed during photolysis and advanced oxidation processes - degradation, elucidation of byproducts and assessment of their biological potency. Chemosphere 85:693–709. https://doi.org/10.1016/j.chemosphere.2011.06.082
24. Vasconcelos TG, Henriques DM, König A, et al (2009) Photo-degradation of the antimicrobial ciprofloxacin at high pH: Identification and biodegradability assessment of the primary by-products. Chemosphere 76:487–493. https://doi.org/10.1016/j.chemosphere.2009.03.022
25. Voigt M, Bartels I, Schmiemann D, et al (2021) Metoprolol and its degradation and transformation products using aops-assessment of aquatic ecotoxicity using qsar. Molecules 26:. https://doi.org/10.3390/molecules26113102
26. Voigt M, Jaeger M (2021) Structure and QSAR analysis of photoinduced transformation products of neonicotinoids from EU watchlist for ecotoxicological assessment. Sci Total Environ 751:141634. https://doi.org/10.1016/j.scitotenv.2020.141634
27. Voigt M, Hentschel B, Theiss N, et al (2020) Lomefloxacin—Occurrence in the German River Erft, Its Photo-Induced Elimination, and Assessment of Ecotoxicity. Clean Technol 2:74–90. https://doi.org/10.3390/cleantechnol2010006
28. Afonso-Olivares C, Montesdeoca-Esponda S, Sosa-Ferrera Z, Santana-Rodríguez JJ (2016) Analytical tools employed to determine pharmaceutical compounds in wastewaters after application of advanced oxidation processes. Environ Sci Pollut Res 23:24476–24494. https://doi.org/10.1007/s11356-016-7325-6
29. Slomberg DL, Ollivier P, Radakovitch O, et al (2017) Insights into natural organic matter and pesticide characterisation and distribution in the Rhone River. Environ Chem 14:64–73. https://doi.org/10.1071/EN16038
30. Uyguner CS, Bekbolet M, Swietlik J (2007) Natural organic matter: Definitions and characterization. Control Disinfect By-Products Drink Water Syst 253–277

31. Fick J, Ph D, Andersson PL, et al (2004) Selection of Antibiotics : A Chemometric Approach . Method. 4th Int Conf Pharm Endocr Disrupting Chem Water 143–150
32. Wold SSM, Eriksson L, Sjöström M, Eriksson L (2001) PLS-regression: A basic tool of chemometrics. Chemom Intell Lab Syst 58:109–130. https://doi.org/10.1016/S0169-7439(01)00155-1
33. Gramatica P, Cassani S, Roy PP, et al (2012) QSAR modeling is not "Push a button and find a correlation": A case study of toxicity of (Benzo-)triazoles on Algae. Mol Inform 31:817–835. https://doi.org/10.1002/minf.201200075
34. Veith GD, Mekenyan OG (1993) A QSAR Approach for Estimating the Aquatic Toxicity of Soft Electrophiles [QSAR for Soft Electrophiles]. Quant Struct Relationships 12:349–356. https://doi.org/10.1002/qsar.19930120402
35. Pavan M, Worth A, Netzeva T (2005) Comparative assessment of QSAR models for aquatic toxicity
36. Kuhn H., Braslavsky SE, Schmidt R (2004) Chemical Actinometry. IUPAC Tech Rep 1–47
37. Hatchard CG, Parker C (1956) A New Sensitive Chemical Actinometer. II. Potassium Ferrioxalate as a Standard Chemical Actinometer. Proc R Soc A Math Phys Eng Sci 235:518–536. https://doi.org/10.1098/rspa.1956.0102
38. Voigt M, Bartels I, Nickisch-Hartfiel A, Jaeger M (2019) Determination of minimum inhibitory concentration and half maximal inhibitory concentration of antibiotics and their degradation products to assess the eco-toxicological potential. Toxicol Environ Chem 0:315–338. https://doi.org/10.1080/02772248.2019.1687706
39. Voigt M, Savelsberg C, Jaeger M (2018) Identification of Pharmaceuticals in The Aquatic Environment Using HPLC-ESI-Q-TOF-MS and Elimination of Erythromycin Through Photo-Induced Degradation. J Vis Exp. https://doi.org/doi:10.3791/57434
40. Voigt M, Bartels I, Nickisch-hartfiel A, Jaeger M (2018) Elimination of macrolides in water bodies using photochemical oxidation. AIMS Environ Sci 5:372–388. https://doi.org/10.3934/environsci.2018.5.372
41. Baghirzade BS, Yetis U, Dilek FB (2021) Imidacloprid elimination by O3 and O3/UV: kinetics study, matrix effect, and mechanism insight. Environ Sci Pollut Res 28:24535–24551. https://doi.org/10.1007/s11356-020-09355-2
42. Lavine BK, Ding T, Jacobs D (2010) LC-PDA-MS studies of the photochemical degradation of imidacloprid. Anal Lett 43:1812–1821. https://doi.org/10.1080/00032711003654013
43. Elumalai P, Yi X, Cai T, et al (2021) Photo-biodegradation of imidacloprid under blue light-emitting diodes with bacteria and co-metabolic regulation. Environ Res 201:111541. https://doi.org/10.1016/j.envres.2021.111541
44. Fernandes CHM, Silva BF, Aquino JM (2021) On the performance of distinct electrochemical and solar-based advanced oxidation processes to mineralize the insecticide imidacloprid. Chemosphere 275:. https://doi.org/10.1016/j.chemosphere.2021.130010
45. Tian J, Rustum A (2018) Development and Validation of a Stability-indicating Reversed-phase UPLC-UV Method for the Assay of Imidacloprid and Estimation of its Related Compounds. J Chromatogr

Sci 56:131–138. https://doi.org/10.1093/chromsci/bmx091

46. Wang Q, Rao P, Li G, et al (2020) Degradation of imidacloprid by UV-activated persulfate and peroxymonosulfate processes: Kinetics, impact of key factors and degradation pathway. Ecotoxicol Environ Saf 187:. https://doi.org/10.1016/j.ecoenv.2019.109779
47. Dell'Arciprete ML, Santos-Juanes L, Sanz AA, et al (2009) Reactivity of hydroxyl radicals with neonicotinoid insecticides: Mechanism and changes in toxicity. Photochem Photobiol Sci 8:1016–1023. https://doi.org/10.1039/b900960d
48. Babic K, Tomašic V, Gilja V, et al (2021) Photocatalytic degradation of imidacloprid in the flat-plate photoreactor under UVA and simulated solar irradiance conditions - The influence of operating conditions, kinetics and degradation pathway. J Environ Chem Eng 9:1–14. https://doi.org/10.1016/j.jece.2021.105611
49. Joice JAI, Aishwarya S, Sivakumar T (2018) Nano Structured Ni and Ru Impregnated TiO 2 Photocatalysts: Synthesis, Characterization and Photocatalytic Degradation of Neonicotinoid Insecticides . J Nanosci Nanotechnol 19:2575–2589. https://doi.org/10.1166/jnn.2019.15880
50. Yin K, Deng Y, Liu C, et al (2018) Kinetics, pathways and toxicity evaluation of neonicotinoid insecticides degradation via UV/chlorine process. Chem Eng J 346:298–306. https://doi.org/10.1016/j.cej.2018.03.168
51. Žabar R, Komel T, Fabjan J, et al (2012) Photocatalytic degradation with immobilised TiO2 of three selected neonicotinoid insecticides: Imidacloprid, thiamethoxam and clothianidin. Chemosphere 89:293–301. https://doi.org/10.1016/j.chemosphere.2012.04.039
52. Sharma T, Kaur M, Sobti A, et al (2020) Sequential microbial-photocatalytic degradation of imidacloprid. Environ Eng Res 25:597–604. https://doi.org/10.4491/eer.2019.150
53. Garg R, Gupta R, Bansal A (2021) Photocatalytic degradation of imidacloprid using semiconductor hybrid nano-catalyst: kinetics, surface reactions and degradation pathways. Int J Environ Sci Technol 18:1425–1442. https://doi.org/10.1007/s13762-020-02866-y
54. Kitsiou V, Filippidis N, Mantzavinos D, Poulios I (2009) Heterogeneous and homogeneous photocatalytic degradation of the insecticide imidacloprid in aqueous solutions. Appl Catal B Environ 86:27–35. https://doi.org/10.1016/j.apcatb.2008.07.018
55. Kurwadkar S, Evans A, DeWinne D, et al (2016) Modeling photodegradation kinetics of three systemic neonicotinoids—dinotefuran, imidacloprid, and thiamethoxam—in aqueous and soil environment. Environ Toxicol Chem 35:1718–1726. https://doi.org/10.1002/etc.3335
56. Moza PN, Hustert K, Feicht E, Kettrup A (1998) Photolysis of imidacloprid in aqueous solution. Chemosphere 36:497–502. https://doi.org/10.1016/S0045-6535(97)00359-7
57. Redlich D, Shahin N, Ekici P, et al (2007) Kinetical study of the photoinduced degradation of imidacloprid in aquatic media. Clean - Soil, Air, Water 35:452–458. https://doi.org/10.1002/clen.200720014
58. Tang J, Huang X, Huang X, et al (2012) Photocatalytic degradation of imidacloprid in aqueous suspension of TiO 2 supported on H-ZSM-5. Environ Earth Sci 66:441–445.

https://doi.org/10.1007/s12665-011-1251-1

59. Wamhoff H, Schneider V (1999) Photodegradation of imidacloprid. J Agric Food Chem 47:1730–1734. https://doi.org/10.1021/jf980820j
60. Wang Y, Sun Q, Tian C, et al (2016) Degradation properties and identification of metabolites of 6-Cl-PMNI in soil and water. Chemosphere 147:287–296. https://doi.org/10.1016/j.chemosphere.2015.12.020
61. Zhang P, Shao Y, Xu X, et al (2020) Phototransformation of biochar-derived dissolved organic matter and the effects on photodegradation of imidacloprid in aqueous solution under ultraviolet light. Sci Total Environ 724:137913. https://doi.org/10.1016/j.scitotenv.2020.137913
62. Agüera A, Almansa E, Malato S, et al (1998) Evaluation of photocatalytic degradation of Imidacloprid in industrial water by GC-MS and LC-MS. Analusis 26:245–251. https://doi.org/10.1051/analusis:1998168
63. Aregahegn KZ, Shemesh D, Gerber RB, Finlayson-Pitts BJ (2017) Photochemistry of Thin Solid Films of the Neonicotinoid Imidacloprid on Surfaces. Environ Sci Technol 51:2660–2668. https://doi.org/10.1021/acs.est.6b04842

Figures

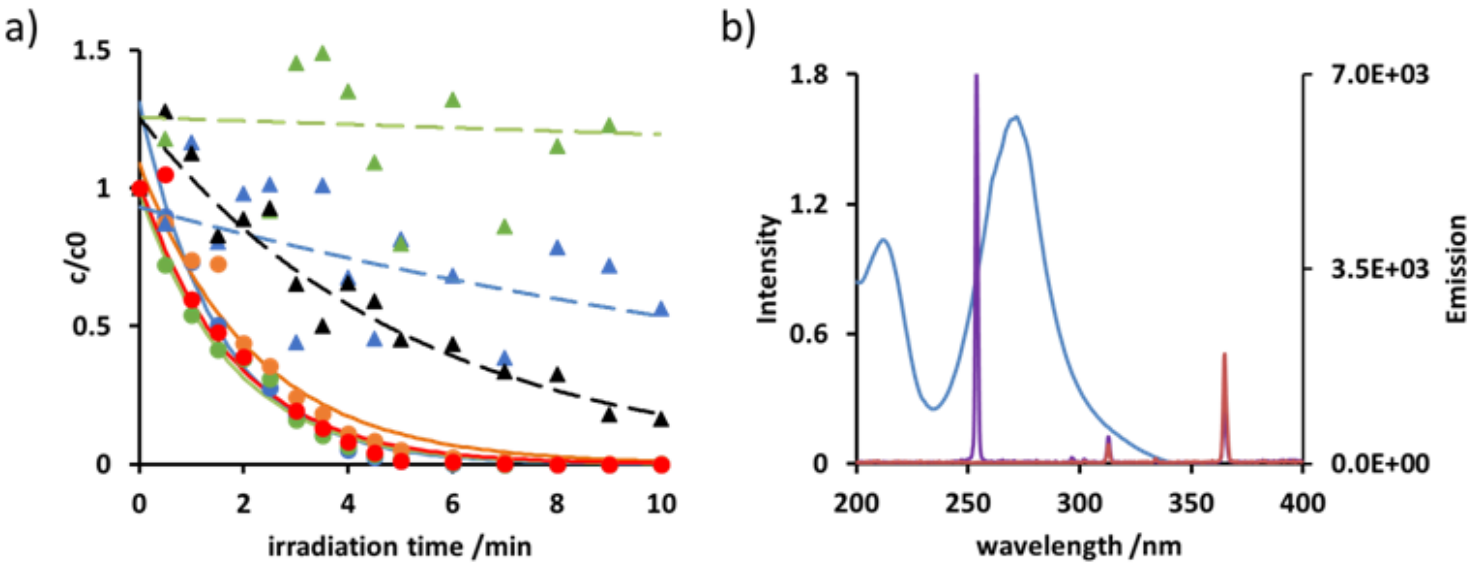

Figure 1

a) Concentration-time curves of photoinduced imidacloprid degradationin ultrapure water (blue), in water containing tert-butanol 5% (green) and 20% (red), in water after addition of 100 mg TiO2 (black) and of 5 mg humic acid (orange)using a UVA lamp (▲) anda VUV/UVC lamp (●); b) emission spectra of the UVA lamp (red), VUV/UVClamp (violet) and absorption spectrum of imidacloprid (blue)

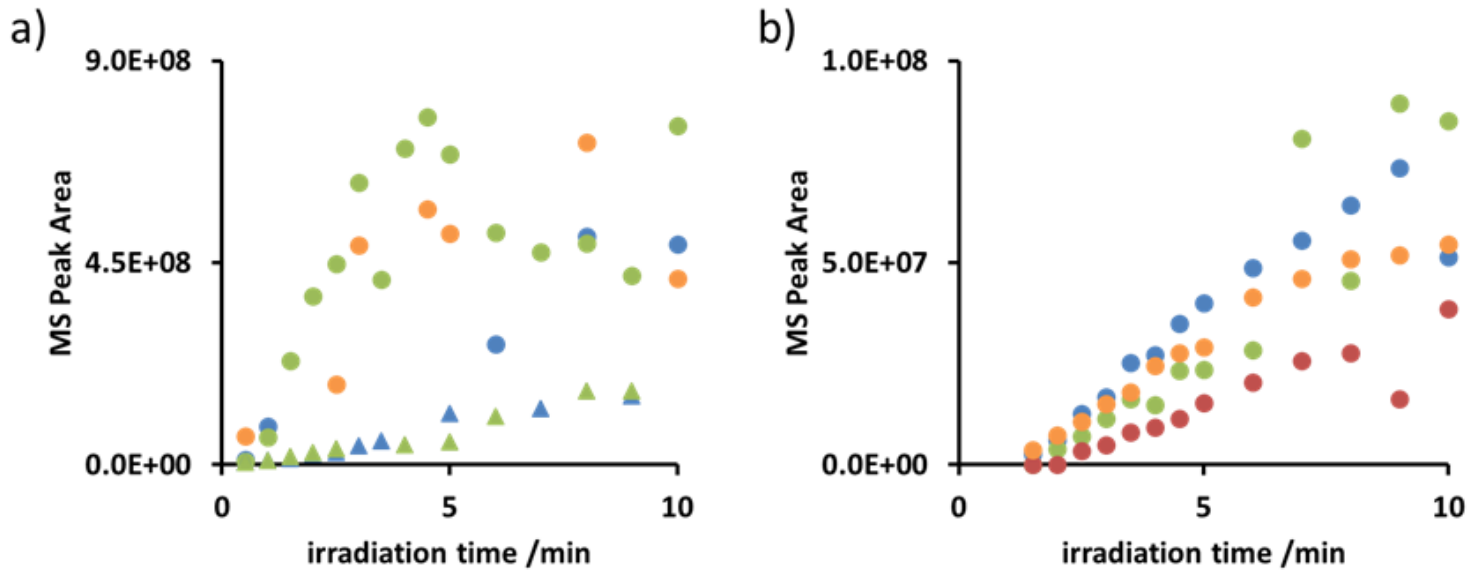

Figure 2

Concentration-time curves of a) desnitroimidacloprid and b) Imi194upon UVA (▲) andVUV/UVC irradiation (●) in water (blue), in the presence oftert-butanol 5% (green), 20% tert-butanol (red), 100 mg TiO2 (violet), and 5 mg humic acid (orange).

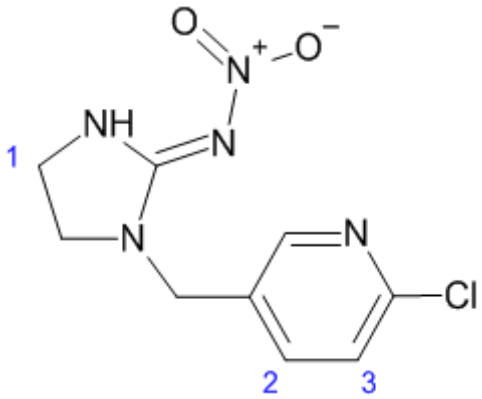

Figure 3

Chemical structure of imidacloprid with hydroxyl position numbering as investigated for ecotoxicity.

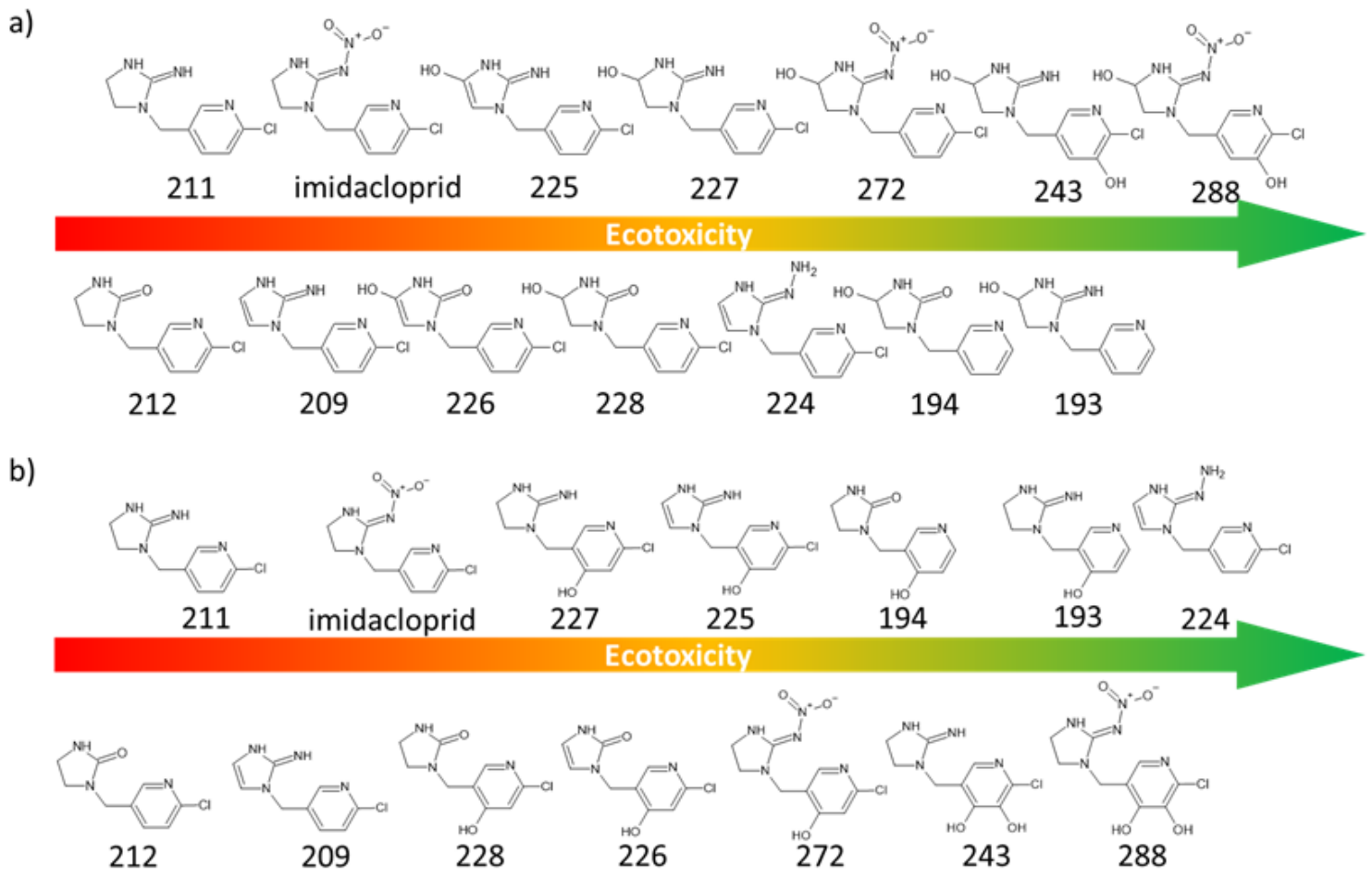

Figure 4

Ranking ofstructures identified during photodegradationaccording to predicted ecotoxicity resulting from QSAR-analysis with hydroxylgroup at position a) 1 and b) 2.

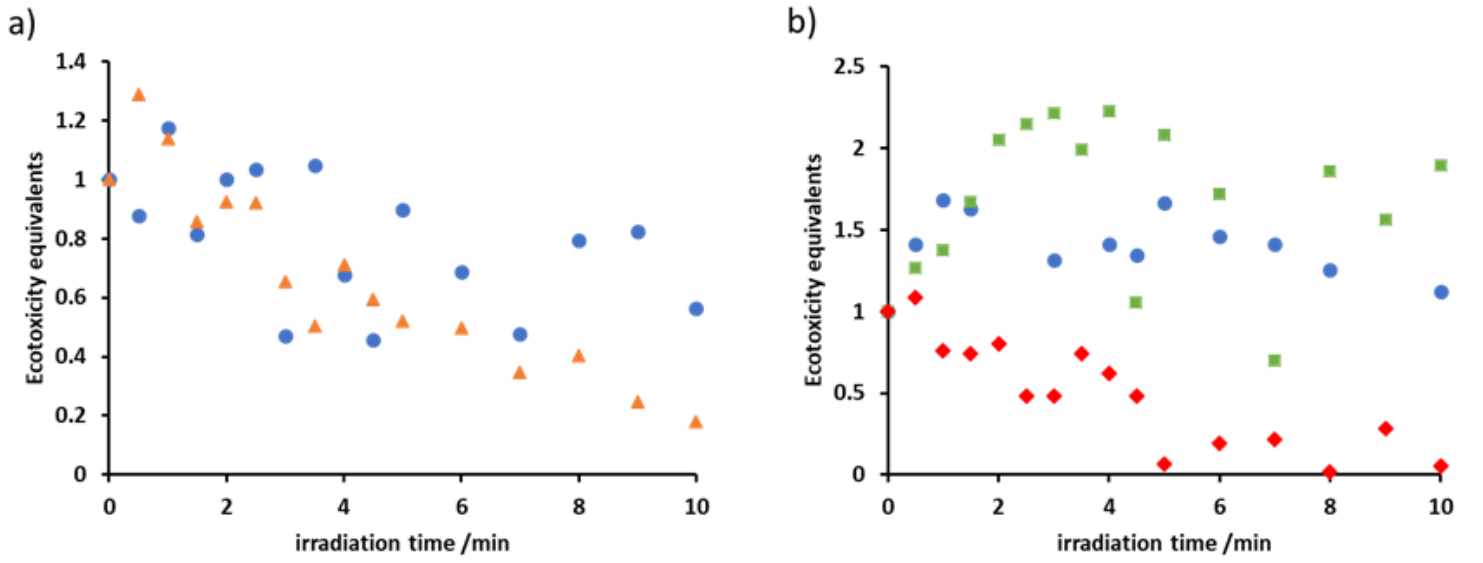

Figure 5

Time-dependent ecotoxicity equivalents of imidacloprid and its photoinduced degradation using a) a UVA lamp and b) a VUV/UVClamp. The degradation experiments were carried out in water (●, blue), with 100 mg TiO2-addition (▲, orange), with 5% tert-butanol (■, green) and 20% tert-butanol (♦, red).

Supplementary Files

This is a list of supplementary files associated with this preprint. Click to download.

- PhotoinduceddegradationofimidaclopridSI3.docx